Selective Binding of a Macrocyclic Bisacridine to DNA Hairpins

A. Slama-Schwok,*,† M.-P. Teulade-Fichou,‡ J.-P. Vigneron,‡ E. Taillandier,† and J.-M. Lehn*,‡

Contribution from the Laboratoire de Spectroscopie Biomoléculaire, URA CNRS 1430, UFR de Santé, Médecine et Biologie Humaine, Université Paris XIII, 74 rue Marcel Cachin, 93012, Bobigny, France, and Chimie des Interactions Moléculaires, UPR 285 CNRS, Collège de France, 11 place Marcelin Berthelot, 75005, Paris, France

Received November 23, 1994[⊗]

Abstract: The reversible hairpin to coil transition of d(GCGAAACGC), named sA_3, was investigated by melting experiments. This oligomer also adopts a bulged duplex structure whose formation from the hairpin is a slow process. The binding of the compound **1**, a macrocycle containing two acridine subunits linked by two diethylenetriamine arms, to the hairpin form was studied using absorption and fluorescence spectroscopy as well as gel filtration. **1** forms two complexes with sA_3 hairpin. The first complex presents a 1/1 **1**/sA_3 stoichiometry, and the binding site of **1** was attributed to the hairpin loop by fluorescence spectroscopy. A similar binding site can be confirmed by the comparison of sA_3 and related hairpins, sA_5, sT_5, and sTAR. The binding constant of **1** for this site is high: $K = (4.5 \pm 0.5) \times 10^7\ M^{-1}$. The second complex presents a 2/1 stoichiometry. The comparison of the hairpin melting temperature in the absence and in the presence of **1** shows a 25 °C stabilization of the hairpin structure by the macrocyclic molecule **1**. In contrast, the reference compound **2**, a monomeric acridine substituted by two propylaminomethyl groups, does not stabilize the hairpin. The results emphasize the selectivity of **1** for the hairpin compared to both double helices and single stranded oligomers arising from its macrocyclic structure. They agree with the initial hypothesis that cage compounds of bicyclointercaland type would bind preferentially to single-stranded than to double-helical nucleic acids domains.

Introduction

Nucleic acids may adopt secondary and tertiary structures, which are sometimes highly conserved. Intramolecular folding of a partially complementary sequence may yield a hairpin, one of the simplest DNA and RNA secondary structures. It is composed by a double helix, the stem, linked to a single-stranded loop. Hairpins are common structural elements in tRNA and mRNA. DNA hairpins are found in gene transcription regions and in origins of DNA replication.[1-3] These structures, forming palindromes, are often recognized by DNA and RNA regulatory proteins.[1,4-8] The possible involvement of DNA hairpins in biological processes led to numerous physical characterization studies of these structures *in vitro*.[9-37] The conformation of hairpin loop containing two to five nucleotides appears to be controlled by many parameters such as the stacking pattern of the loop residues over the stem, the steric constraint for loop closure, the interactions of the loop bases between themselves including stacking and/or hydrogen bond formation, and the identity of the stem closing pair.[9-37]

It is of interest to develop compounds that may act as probes of nucleic acids. The two main approaches to the design

† Université Paris XIII.

‡ Collège de France.

[⊗] Abstract published in *Advance ACS Abstracts,* June 1, 1995.

(1) (a) McMurray, C. T.; Wilson, W. D.; Douglass, J. O. *Proc. Natl. Acad. Sci. U.S.A.* **1991**, *88*, 666−670. (b) Spiro, C.; Richards, J. P.; Chandrasekaran, R. G.; Brennan, R. G.; McMurray C. T. *Proc. Natl. Acad. Sci. U.S.A.* **1993**, *90*, 4606−4610.

(2) Ohshima, A.; Inouye, S.; Inouye, M. *Proc. Natl. Acad. Sci. U.S.A.* **1992**, *89*, 1016−1020.

(3) Miao, D.-M.; Honda, Y.; Tanaka, K.; Higashi, A.; Nakamura, T.; Taguchi, Y.; Sakai, H.; Komano, T.; Bagdasarian, M. *Nucl. Acid Res.* **1993**, *21*, 4900−4903.

(4) Fourcade-Peronnet, F.; Codani-Simonart, S.; Best-Belpomme, M. *J. Virology* **1992**, *66*, 1682−1687.

(5) Sun, W.; Godson, G. N. *J. Biol. Chem.* **1993**, *268*, 8026−8039.

(6) (a) Berkhout, B.; Gatignol, A.; Rabson, A. B.; Jeang, K. T. *Cell* **1989**, *62*, 757−767. (b) Marciniak, R. A.; Garcia-Blanco, M. A.; Sharp, P. A. *Proc. Natl. Acad. Sci. U.S.A.* **1990**, *87*, 3624−3628.

(7) Heaphy, S.; Finch, J. T.; Gait, M. J.; Karn, J.; Singh, M. *Proc. Natl. Acad. Sci. U.S.A.* **1991**, *88*, 7366−7370.

(8) Hehl, A.; Vassella, E.; Braun, R.; Roditi, I. *Proc. Natl. Acad. Sci. U.S.A.* **1994**, *91*, 370−374.

(9) Altona, C.; van Beuzekom, A. A.; Orbons, L. P. M.; Pieters, J. M. L. In Biological and artificial intelligence systems: Clementi, E., Chin, S., Eds., Escom: Leiden, 1988, pp 93−124.

(10) Chattopadhyaya, R.; Ikuta, S.; Grzeskowiak, K.; Dickerson, R. E. *Nature* **1988**, *334*, 175−179.

(11) Chattopadhyaya, R.; Grzeskowiak, K.; Dickerson, R. E. *J. Mol. Biol.* **1990**, *211*, 189−210.

(12) Hare, D. R.; Reid, B. R. *Biochemistry* **1986**, *25*, 5341−5350.

(13) Haasnoot, C. A. G.; de Bruin, S. H.; Berendsen, R. G.; Janssen, H. G. J. M.; Binnendijk, T. J. J.; Hilbers, C. W.; van der Marel, G. A.; van Boom, J. H. *J. Biomol. Struct. Dyn.* **1983**, *1*, 115−129.

(14) Haasnoot, C. A. G.; Hilbers, C. W.; van der Marel, G. A.; van Boom, J. H.; Singh, U. C.; Pattabiraman, N.; Kollman, P. A. *J. Biomol. Struct. Dyn.* **1986**, *3*, 843−857.

(15) Ikuta, S.; Chattopadhyaya, R.; Ito, H.; Dickerson, R. E.; Kearns, D. R. *Biochemistry* **1986**, *25*, 4840−4849.

(16) Germann, M. W.; Kalisch, B. W.; Lundberg, P.; Vogel, H. J.; van de Sande, H. *Nucl. Acid Res.* **1990**, *18*, 1489−1498.

(17) Pramnik, P.; Kanhouwa, N.; Kan, L.-S. *Biochemistry* **1988**, *27*, 3024−3031.

(18) Blommers, M. J. J.; Walters, A. L. I.; Haasnoot, C. A. G.; Aelen, J. M. A.; van der Marel, G. A.; van Boom, J. H.; Hilbers, C. W. *Biochemistry* **1989**, *28*, 7491−7498.

(19) Xodo, L. E.; Manzini, G.; Quadrifoglio, F.; van der Marel, G. A.; van Boom, J. *Biochemistry* **1988**, *27*, 6321−6326.

(20) Pieters, J. M. L.; de Vroom E.; van der Marel, G. A.; van Boom, J. H.; Koning, T. M. G.; Kaptein, R.; Altona, C. *Biochemistry* **1990**, *29*, 788−799.

(21) Boulard, Y.; Gabarro-Arpa, J.; Le Bret, M.; Guy, A.; Téoulé, R.; Guschlbauer, W.; Fazakerley, G. V. *Nucl. Acid. Res.* **1991**, *19*, 5159−5167.

(22) Xodo, L. E.; Manzini, G.; Quadrifoglio, F.; van der Marel, G.; van Boom, J. H. J. *Nucl. Acid. Res.* **1991**, *19*, 1505−1511.

(23) McMurray, C. T.; Wilson, W. D.; Douglass, J. O. *Proc. Natl. Acad. Sci. U.S.A.* **1991**, *88*, 666−670.

(24) Groebe, D. R.; Uhlenbeck, O. C. *Nucl. Acid Res.* **1988**, *16*, 11725−11735.

(25) Sakata, T.; Hiroaki, H.; Tanaka, T.; Ikehara, M.; Uesugi, S. *Nucl. Acid Res.* **1990**, *18*, 3831−3839.

0002-7863/95/1517-6822$09.00/0

Scheme 1

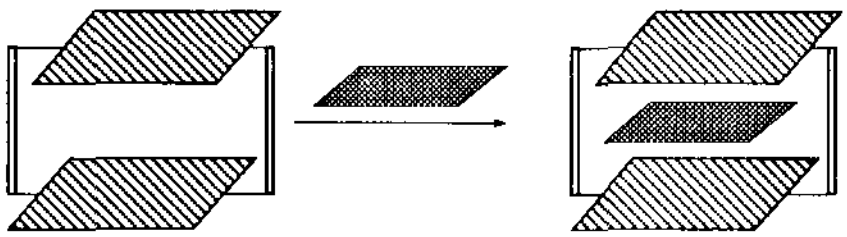

Cyclo-intercalation

The substrat, schematized as a grey rectangle, can be a single-stranded portion of DNA or a small flat molecule.

of artificial agents for nucleic acid recognition involve the following:

(1) *sequence selective compounds*, for which the goal is to target precisely a well-defined and identified site in a nucleic acid and

(2) *structural probes* destined to provide a general method for detecting a given type of structural feature (single-strand, double-strand, loop, bulge, etc.).

Numerous studies have been conducted along these two lines, leading to more or less efficient and specific targeting procedures. In addition, the combination with chemically reactive groups permits to perform reactions at specific sites of a nucleic acid. A limited number of synthetic compounds have been designed to probe the secondary and tertiary structure of DNA and RNA. $Rh(phen)_2ph^{3+}$ promotes strand cleavage at sites of tertiary interaction in t-RNA.[38] Ni(II) macrocyclic complexes detect and cleave guanine bases in mismatches, bulges and loops.[39]

Several synthetic molecules bind on DNA hairpin stem. For instance, ethidium bromide is preferentially intercalated between G−C pairs of the $(GC)_2T_n(GC)_2$ hairpin.[41] Actinomycin D also binds via intercalation at the single d(GC) step of an hairpin stem.[41] Netropsin stabilizes a dumbbell structure by binding into the stem minor groove.[42] Compounds of the enediyne antibiotics family present cleavage properties at flexible regions of DNA such as bulges.[43,44] The neocarzinostatin chromophore selectively cleaves DNA containing a bulged T structure via a thiol-independent mechanism.[43] Intercalators linked to an appropriate nucleic acid base bind to bulged duplexes.[45]

We have been interested in developing nucleic acid recognition probes that may discriminate between single- and double-stranded domains. Our approach involves a general type of structures, the cyclo-bis-intercaland macrocycles incorporating two intercalator subunits linked by two bridges. The basic concept was that the structural features of such cage-like molecules would disfavor their binding to double-stranded nucleic acid domains but allow their interaction with single-stranded sequences (Scheme 1).

Several types of such cyclo-bis-intercalands have been synthesized, and their ability to complex various molecular substrates including nucleic acid compounds has been investigated.[46-51] It has been shown that a porphyrin cage compound binds preferentially to single-stranded nucleic acid domains and effects photocleavage under irradiation with visible light.[46,47]

Various bisintercalators and polyintercalators including bisacridines have been previously synthesized. The interest in such compounds arise from their high affinity to DNA duplexes and the anticancer activity of some of these molecules. These compounds promote substantial changes in DNA conformation induced by the intercalation process.[52-55] The binding of a macrocyclic bisacridine to DNA duplex has been previously described.[54]

We now report a study of the interaction of the cyclo-bisacridine compound **1**[56] with the oligonucleotide d(GCG AAA CGC). This oligomer, named sA_3 where s designates the stem sequence, was designed for providing loop and bulge superstructures. The bisacridine **1** possesses flexible arms, which are positively charged to insure electrostatic attraction with the

(26) (a) Puglisi, J. D.; Wyatt, J. R.; Tinoco, I., Jr. *Biochemistry* **1990**, *29*, 4215−4226. (b) Varini, G.; Cheong, C.; Tinoco, I., Jr. *Biochemistry* **1991**, *30*, 3280−3289.

(27) SantaLucia, J.; Kierzek, R.; Turner, D. H. *Biochemistry* **1991**, *30*, 8242−8252.

(28) Uhlenbeck, O. C. *Nature* **1990**, *346*, 613.

(29) SantaLucia, J.; Kierzek, R.; Turner, D. H. *Science* **1992**, *256*, 217−219.

(30) Heus, H. A.; Pardi, A. *Science* **1991**, *253*, 191−193.

(31) Antao, V. P.; Tinoco, I., Jr. *Nucl. Acid Res.* **1992**, *20*, 819−824 and 5901−5909.

(32) Hirao, I.; Nishimura, Y.; Tagawa, Y.; Watanabe, K.; Miura, K. *Nucl. Acid Res.* **1992**, *20*, 3891−3896.

(33) Williamson, J. R.; Boxer, S. G. *Biochemistry* **1989**, *28*, 2819−2831 and 2831−2836.

(34) Senior, M. M.; Jones, R. A.; Breslauer, K. J. *Proc. Natl. Acad. Sci. U.S.A.* **1988**, *85*, 6242−6246.

(35) Baxter, S. M.; Geierstein, M. B.; Kushlan, D. M.; Ashley, G. W. *Biochemistry* **1993**, *32*, 8702−8711

(36) Paner, T. M.; Amaratunga, M.; Benight, A. S. *Biopolymers* **1992**, *32*, 881−892.

(37) Paner, T. M.; Amaratunga, M.; Benight, A. S. *Biopolymers* **1992**, *32*, 1715−1734.

(38) Chow, C. S.; Behlen, L. S.; Uhlenbeck, O. C.; Barton, J. K. *Biochemistry* **1992**, *31*, 972−982.

(39) (a) Chen, X.; Burrows, C. J.; Rokita, S. E. *J. Am. Chem. Soc.* **1992**, *114*, 322−325. (b) Muller, J. G.; Chen, X.; Dadiz A. C.; Rokita, S. E.; Burrows, C. J. *J. Am. Chem. Soc.* **1992**, *114*, 6407−6411.

(40) Rentzeperis, D.; Alessi, K.; Marky, L. A. *Nucl. Acid Res.* **1993**, *21*, 2683−2689.

(41) Brown, D. R.; Kurz, M.; Kearns, D. R.; Hsu, V. L. *Biochemistry* **1994**, *33*, 651−664.

(42) Rentzeperis, D.; Ho, J.; Marky, L. A. *Biochemistry* **1993**, *32*, 2564−2572.

(43) Kappen, L. S.; Goldberg, I. H. *Biochemistry* **1993**, *32*, 13138−13145.

(44) Kusakabe, T.; Maekawa, K.; Uesugi, M.; Sugiura, Y. *Biochemistry* **1993**, *32*, 11669−11675.

(45) Wilson, W. D.; Ratmeyer, L.; Cegla, M. T.; Spychala, J.; Boykin, D.; Demeunynck, M.; Lhomme, J.; Krishnan, G.; Kennedy, D.; Vinayak, R.; Zon, G. *New J. Chem.* **1994**, *18*, 419−423.

(46) Slama-Schwok, A.; Lehn, J.-M. *Biochemistry* **1990**, *29*, 7895−7903

(47) Blacker A. J. Thèse de Doctorat de l'Université Louis Pasteur de Strasbourg, 1988.

(48) Jazwinski, J.; Blacker, A. J.; Lehn, J.-M.; Cesario, M.; Guilhelm, J.; Pascard, C. *Tetrahedron Lett.* **1987**, *28*, 6057−6060.

(49) (a) Lehn, J.-M.; Schmidt, F.; Vigneron, J.-P. *Tetrahedron Lett.* **1988**, *29*, 5255−5258. (b) Claude S., Lehn J.-M., Vigneron J.-P. *Tetrahedron Lett.* **1989**, *30*, 941−944.

(50) Zinic, M.; Cudic, P.; Vigneron, J.-P.; Lehn J.-M. *Tetrahedron Lett.* **1992**, *33*, 7417−7420.

(51) Dhaenens, M.; Lehn, J.-M.; Vigneron, J.-P. *J. Chem. Soc., Perkin Trans.* **1993**, *2*, 1379−1381.

(52) (a) Le Pecq, J.-B; Le Bret, M.; Barbet, J.; Roques, B. *Proc. Natl. Acad. Sci. U.S.A.* **1975**, *72*, 2915−2919. (b) Pelprat, D.; Delbarre, A.; Le Guen, I.; Roques, P. B.; Le Pecq, J.-B *J. Med. Chem.* **1980**, *23*, 1336−1343. (c) Laugaa, P.; Markovits, J.; Delbarre, A.; Le Pecq, J.-B; Roques, P. B. *Biochemistry* **1985**, *24*, 5567. (d) Delbarre, A.; Delepierre, M.; Garbay, C.; Igolen, J.; Roques, P. B.; Le Pecq, J.-B *Proc. Natl. Acad. Sci. U.S.A.* **1987**, *84*, 2155−2159. (e) Laugaa, P; Delepierre, M.; Dupraz, B.; Igolen, J.; Roques, P. B. *J. Biomol. Struct. Dyn.* **1988**, *6*, 421−441. (f) Delepierre, M.; Maroun, R.; Garbay-Jaureguiberry, C.; Igolen, J.; Roques, P. B. *J. Mol. Biol.* **1989**, *210*, 211−228. (g) Markovits, J.; Garbay-Jaureguiberry, C.; Roques, P. B.; Le Pecq, J.-B. *Eur. J. Biochemistry.* **1989**, *180*, 359−366.

Chart 1

Tetracationic form of the macrocyclic bis-acridine **1** at pH = 6.0

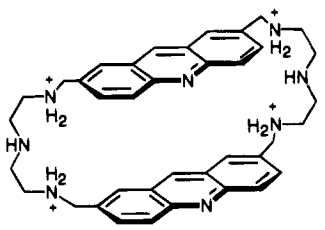

Monomeric reference compound **2**

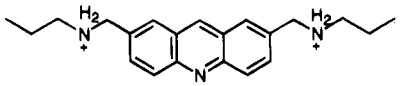

phosphate groups, and two uncharged acridine moieties that may stack on loop bases (Chart 1). These effects are responsible for the strong complexation of mononucleotides.[56] This bulky molecule should not intercalate into the stem, as other acridine derivatives, due to steric hindrance. The influence of steric effects can be evaluated by comparing the macrocyclic acridine **1** with its reference monomeric compound **2**.[56]

The results presented in this work are consistent with a high affinity and a selectivity of the macrocyclic acridine **1** for the hairpin structure.

Experimental Section

1. Materials. The oligonucleotides GCG(AAA)CGC, GCG-(AAAAA)CGC, GCG(TTTTT)CGC and GCG(CTGGGA)CGC, referred to as sA_3, sA_5, sT_5, and sTAR respectively, s representing the stem sequence, were purchased from Genosys or Appligene. The samples were purified by HPLC, ethanol precipitated, and then desalted on a Sephadex G-10 column. The tetramer $d(A)_4$ was purchased from Appligene. The oligonucleotide dA_3 was synthesized in the laboratory of Prof. V. Vlassov at the Molecular Biology Institute of the Siberian Academy of Sciences, Novosibirsk. The oligomer dA_{20} and the polynucleotides polyd(A-T), polydT, and polyd(G-C) were purchased from Pharmacia. The chemicals used were of the highest commercial purity. The solutions contained 1 mM cacodylate buffer, 4 mM NaCl at pH = 6.0 unless otherwise stated. All aqueous solutions utilized purified water (MilliQ, Millipore). The synthesis of the macrocyclic acridine **1** and of the reference acridine compound **2** has been previously reported.[56]

2. Melting Temperature Measurements. The T_m measurements were performed with a Kontron 941 spectrophotometer. The temperature of the six-cell holder was regulated by circulating water using a Haake cryothermostat and controlled by a temperature sensor (thermiresistor) immersed within a reference cell containing appropriate buffer. Constant heating or cooling rates were obtained using a Haake PG20 temperature programmer. The rate of temperature change was usually (0.05−0.1) °C/ min. T_m values were calculated by the first derivative of the melting curves. Various cell path-lengths ranging from 1 to 0.2 cm were used depending on the oligomer concentration, so the measured absorbance did not exceed 1.7 OD.

The melting profiles of sA_3 were monitored at 280, 275, 257, and 246 nm with the oligonucleotide alone and at 280 and 362 or 359 nm in the presence of **1** or **2**. **1** and **2** present a large absorption peak at 247 nm. The 280 nm wavelength was chosen with respects to the lowest contribution of **1** to the total absorption in the concentration range used [**1**] = 1−40 μM based on ε values of free **1** and **2**. Full absorption spectra at various temperatures were also recorded to determine the presence of isosbestic points.

The oligonucleotide samples used for melting experiments were slowly heated to 90 °C for 30 min, then gently cooled to 3 °C, and stored for 48 h at this temperature before measurement. Experiments in the presence of the macrocyclic acridine **1** (or the reference compound **2**) were performed in the following way: **1** was added within the cell containing the denaturated sA_3 at 75 °C, and then the solution was slowly cooled and stored 24 h for equilibration before measurement. Both compounds **1** and **2** did not present any degradation over repeated heating and cooling cycles.

3. Fluorescence Measurements. The fluorescence measurements were performed with a Fluoromax apparatus (Spex) equipped with an Hamamatsu 928 photomultiplier, using a thermostated cell holder. The data have been corrected for the response of the PM and the variation of the absorption at the excitation-wavelength. Relative fluorescence yields were obtained using quinine sulfate and anthracene as references. Repeated fluorescence measurements of **1** complexed to sA_3 induce spectral modifications under continuous 360 nm irradiation possibly due to a photochemical reaction. This was avoided by taking short integration times and small excitation pathlengths l = 0.4 cm.

4. Chromatography. The complexes of **1** with the DNA hairpin have been studied by gel filtration using a Sephadex G-10 column. The resin was equilibrated in the above buffer and carefully washed with about 10 column volumes before loading the oligonucleotide sample (1 mL at 10 mM) with or without the macrocyclic acridine **1**. The absorption and fluorescence spectra of the eluted 0.5 mL fractions were then measured.

Results

1. Melting Profile of the Oligonucleotide GCGAAACGC named sA_3, comparison with sA_5, sT_5, and sTAR. Figure 1 shows typical absorbance versus temperature profiles of GCG AAA CGC, named sA_3, where s designates the stem sequence. Two transitions are observed at [sA_3] = 40 μM, [NaCl] = 4 mM. They are called transitions 1 and 2, occurring at lower and higher temperature respectively.

The melting temperature, "T_m1", of transition 1 depends on the oligonucleotide concentration. This transition is not reversible on the time scale of the T_m measurements: the initial absorbance is restored only after ca. 2 days at 4 mM NaCl, [sA_3]= 10 μM, and 15 °C, and the recovery time depends on sA_3 concentration. Therefore, "T_m1" is an apparent value of T_m1 at this [NaCl].

The melting temperature of transition 2, T_m2 = (47 ± 1) °C, is unchanged by a 50-fold increase in oligonucleotide concentration, (1−50) μM (in strand). This transition is reversible and covers a broad temperature range with a van't Hoff enthalpy $\Delta H = -(19 \pm 2)$ Kcal/mol and $\Delta S = -(59 \pm 5)$ eu; ΔH and ΔS are calculated from the UV melting curves using the renaturation curve to avoid transition 1, assuming a two-state model.

(53) (a) Wakelin, L. P. C.; Romanos, M.; Chen, T. K.; Canellakis, E. S.; Waring, M. J. *Biochemistry* **1978**, *17*, 5057−5063. (b) Denny, W. A.; Atwell, G. J.; Baguley, B. C.; Wakelin, L. P. C. *J. Med. Chem.* **1985**, *28*, 1568−1574. (c) Assa-Nuria, N.; Denny, W. A.; Leupin, W.; Kearns, D. R. *Biochemistry* **1985**, *24*, 1441−1449. (d) Wakelin, L. P. C. *Med. Res. Rev.* **1986**, *6*, 275−340. (e) Denny, PW. A.; Atwell, G.; Willmott, G. A.; Wakelin, L. P. C. *Biophys. Chem.* **1985**, *22*, 17−26. (f) Atwell, G. J.; Baguley, B. C.; Wilmanska, D.; Denny, W. A. *J. Med. Chem.* **1986**, *29*, 69−74.

(54) (a) Zimmerman, S. C.; Lamberson, C. R.; Cory, M.; Firley, T. A. *J. Am. Chem. Soc.* **1989**, *111*, 6805−6809. (b) Veal, J. M.; Zimmerman, S. C.; Lamberson, C. R.; Cory, M.; Zon, G.; Wilson, W. D. *Biochemistry* **1990**, *29*, 10918−10927. (c) Eggert, H.; Dinesen, J.; Jacobsen, J. P. *Biochemistry* **1989**, *28*, 3332−3337.

(55) (a) Delbarre, A.; Brown, S. C.; James, T. L.; Shafer, R. H. *Biopolymers* **1988**, *27*, 1953−1975. (b) Mullins, S. T.; Annan, N. K.; Cook, P. R.; Lowe, G. *Biochemistry* **1992**, *31*, 842−849. (c) Annan N. K., Mullins S. T., Lowe G. *Nucl. Acid Res.* **1992**, *20*, 983−990.

(56) Teulade-Fichou, M.-P.; Vigneron, J.-P.; Lehn, J.-M. *J. of Supramolecular Chem.*, in press.

Similar melting behaviors have been reported[9,19,21,22,57] and attributed to the following:

—a slow intermolecular transition from a bulged duplex to an hairpin form, corresponding to transition 1 in agreement with slower kinetics of the hairpin to duplex interconversion reported for "blunt end" palindromes compared to that for dangling ended ones[57] and

—a fast intramolecular transition from a hairpin to a random coil, corresponding to transition 2.

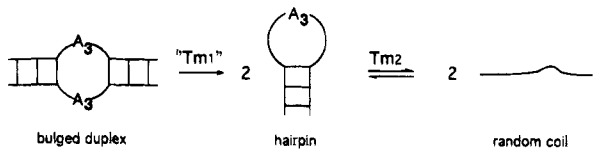

Besides the independence of the T_m2 on the oligonucleotide concentration, the effect of salt concentration on the melting temperature is useful to characterize the hairpin form.[40,42,58,59] A shift of T_m2 from 41.7 to 55 °C is observed as [NaCl] is increased from 1 to 200 mM, using [sA_3] = 10 μM. The plot of T_m2 versus log[NaCl] has a slope $dT_m/d\log[Na^+]$ = (5.1 ± 0.4) °C. This dependence on salt concentration is similar to the value of 4.7 °C found with the hairpin $(G\text{-}C)_2T_5(G\text{-}C)_2$.[40,59] The salt-dependence measurements allow to estimate the thermodynamic counterion release, Δn, of transition 2, based on the above assumption of a two-state model:

$$dT_m/d\log[Na^+] = -0.9(2.303RT_m^2/\Delta H°)\Delta n$$

A value of Δn = 0.229 is obtained, corresponding to a counterion release per phosphate Δi = 0.0286 (including both the helical stem and loop phosphates). This last value is in good agreement with Δi = 0.021−0.031 and 0.027, characteristic of the ion release process in the melting of small DNA hairpins.[40,42,58,59]

The concentration independence of transition 2 as well as its salt dependence are both consistent with its attribution to the intramolecular hairpin to coil interconversion.

The melting profiles of the oligonucleotides sA_5, sT_5, and sTAR have been measured, and the T_m values were found to be independent of the strand concentration as expected for an intramolecular transition from hairpin to random coil structures. The T_m2 values obtained for sA_5, sT_5, and sTAR are, respectively, (35 ± 2) °C, (40 ± 2) °C and (45 ± 2) °C. The sT_5 hairpin presents a higher stability than sA_5 in agreement with published data on A_n and T_n hairpin loops with homologous stem sequence.[22,28,31,60] The decreasing stability from T_m2 = (47 ± 1) to T_m2 = (35 ± 2) °C while increasing loop size from 3 to 5 adenines follows the same trend than other DNA hairpins within similar series.[19,20,22,32,58]

No clear evidence for another transition (at lower temperature) is detected for sT_5 and sTAR. A small transition is observed around 17 °C for [sA_5] = 10 μM, pointing out at the existence of a bulged duplex structure at low temperature.

II. Binding of the Macrocyclic Acridine 1 to sA_3 and to Model Oligonucleotides. (a) The Macrocyclic Acridine Fluorescence Is Sensitive to DNA Structure. 1. Oligonucleotide sA_3. The absorption spectrum of the macrocyclic acridine is modified when bound in the presence of an excess of sA_3: a large hypochromism, D/D_0 (362) = 0.7, is observed together with a slight 2 nm red-shift compared to free **1** (λ_{max} = 360 nm).

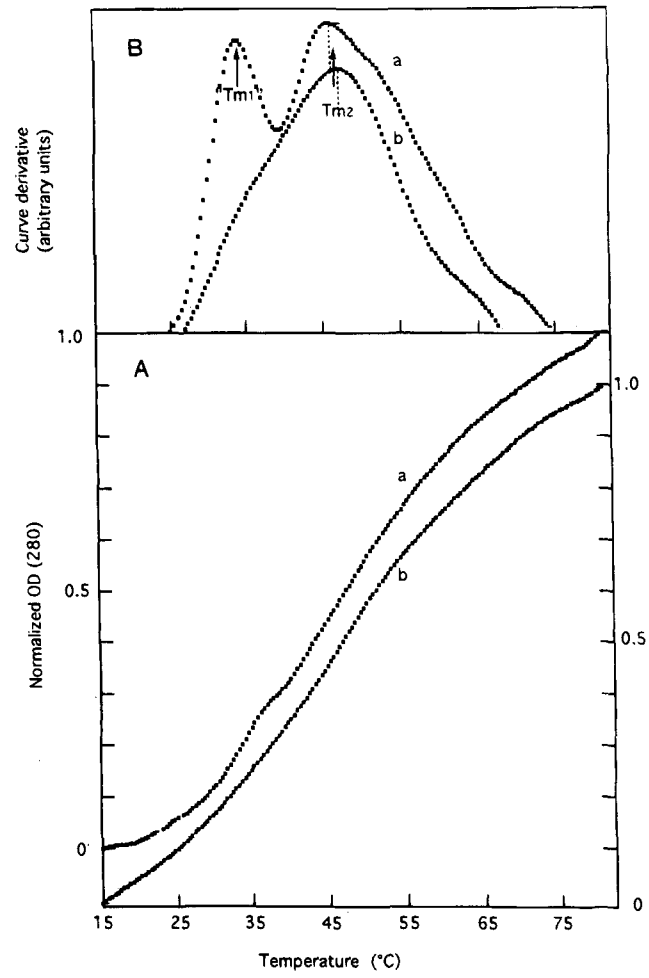

Figure 1. Effect of sA_3 concentration on its melting profile; 4 mM NaCl, 1 mM cacodylate buffer pH = 6.0; (A) the two melting curves, monitored at 280 nm, have been shifted for clarity; a and b: left and right scale respectively; (B) first derivative of the melting curves; b: [sA_3] = 2 μM (in strand), pathlength l = 1 cm; a: [sA_3] = 40 μM, l = 0.4 cm.

The binding of the bisacridine to excess sA_3 induces clear modifications of its fluorescence spectrum, shown in Figure 2. The maximum is red-shifted from 433 to 441 nm, and the overall shape is modified from a broad unstructured peak to well resolved vibronic bands. Two bands are observed at [NaCl] = 4 mM, whereas an additional broad shoulder at 470 nm is present at [NaCl] = 500 mM. This modification of the fluorescence spectrum may be attributed to a change in the structural environment of **1**, induced by [NaCl] increase that shifts the duplex to hairpin equilibrium toward the former. The melting temperature for the first transition is observed at about 35 °C at 500 mM NaCl and [sA_3] = 2 μM strand, pointing out that the bulged duplex is the predominant structure in these conditions.

2. Double-Stranded DNA. The above results suggest that the macrocyclic acridine fluorescence maximum may be sensitive to the nucleic acid structure. This hypothesis was first tested with double stranded DNAs. Fluorescence maxima are observed between 470 and 480 nm, similar for all double stranded polynucleotides tested (see Table 1). This is quite a large red-shift, of about 42 nm, relative to free **1**. A comparable result was also obtained for an oligonucleotide duplex named {G_2-

(57) Xodo, L. E.; Manzini, G.; Quadrifoglio, F.; Yathindra, N.; van der Marel, G.; van Boom, J. *J. Mol. Biol.* **1989**, *205*, 777−781.

(58) Marky, L. A.; Blumenfeld, K. S.; Kozlowsky, S.; Breslauer, K. J. *Biopolymers* **1983**, 1247−1257.

(59) Rentzeperis, D.; Kharakoz, D. P.; Marky, L. A. *Biochemistry* **1991**, *30*, 6276−6283.

(60) Baumann U.; Frank, K.; Blöcker, H. *Eur. J. Biochem.* **1986**, 409−413.

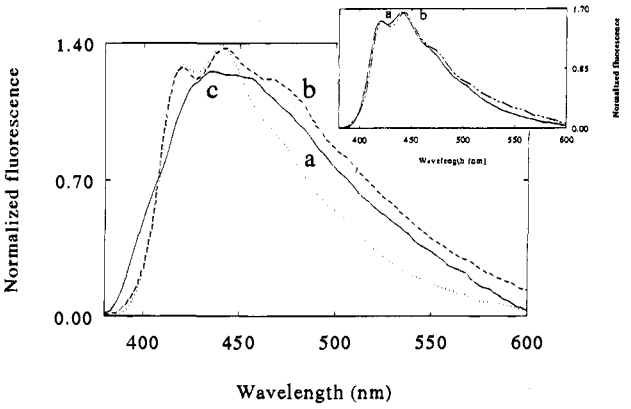

Figure 2. Effect of NaCl concentration on the normalized fluorescence spectra of the macrocyclic acridine bound to sA_3; $[sA_3] = 40\ \mu M$, [**1**] = 5 μM, 1 mM cacodylate buffer pH = 6.0, excitation wavelength λ = 360 nm, excitation and emission slits:1.15 nm; a: [NaCl] = 4 mM, b: [NaCl] = 500 mM, c: free **1** at 4 mM NaCl; insert: normalized fluorescence spectra of the macrocyclic acridine **1** bound to AMP and to sA_3 hairpin. a: [AMP] = 10 μM, b: $[sA_3] = 40\ \mu M$. [**1**] = 5 μM.

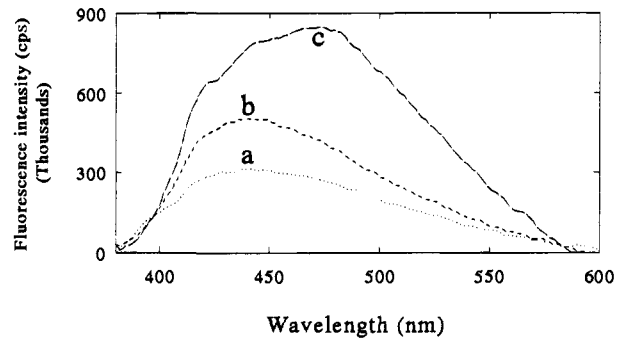

Figure 3. Comparison of the fluorescence spectra of **1** bound to single stranded and double stranded oligomers; a: $[G_2] = 50\ \mu M$, b: $[C_2] = 50\ \mu M$, c: $[\{G_2\text{-}C_2\}] = 25\ \mu M$, excitation wavelength λ = 360 nm, excitation and emission slits: 1.15 nm.

$C_2\}$, obtained from the 1/1 mixture of G_2 and C_2 oligomers, the 5′3′ and 3′5′ strands of $\{G_2\text{-}C_2\}$ respectively. This model duplex represents a kind of mimic of one sA_3 stem:

$$5'\ GCGGCG\ 3'\ G_2$$

$$3'\ CGCCGC\ 5'\ C_2$$

A c.a 42 nm red-shift of λ_{max} seems thus to characterize **1** in a double-stranded environment.

3. Single-Stranded DNA and sA_5, sT_5, and sTAR Hairpins. Figure 3 shows the fluorescence spectrum of **1** bound to the above double-helical $\{G_2\text{-}C_2\}$ compared to that observed in the presence of each of its strands, G_2 and C_2. The fluorescence maxima of **1** are found at 443 nm when bound to both single-stranded oligomers, the two strands of $\{G_2\text{-}C_2\}$, whereas for the duplex bound macrocycle, the fluorescence peaks at 475 nm. This result confirms the above hypothesis stating that the macrocycle fluorescence is sensitive to DNA structure. Namely, the data point out that a duplex environment results in a (475 ± 5) nm fluorescence maximum.

The question is then whether the fluorescence maxima of bound **1** are sensitive to single-stranded oligomers sequence. If this is the case, the data may allow the deducing of the macrocycle binding site in sA_3 hairpin. Table 1, Figure 2 (insert), and Figure 4A compare the macrocyclic acridine fluorescence bound to sA_3 and sA_5 hairpins, AMP, dA_3, and dA_{20}. The fluorescence spectra peak at (441 ± 2) nm for all the adenine oligomers including sA_3 and sA_5.

Table 1 . Fluorescence Maxima and Relative Yields for the Macrocyclic Acridine **1** Bound to Various Oligo- and Polynucleotides

DNA	λ_{max} (± 1 nm)	Φ/Φ_0[b]
AMP	440	0.8 ± 0.1
dA_3	440	0.5 ± 0.05
dA_4	440	0.7 ± 0.1
dA_{20}	442	0.9 ± 0.1
sA_3	441	6.8 ± 0.5
sA_5	442	0.7 ± 0.1
dT_4	425	6.8 ± 0.3
polydT	425	7.2 ± 0.3
sT_5	427	1.0 ± 0.1
sTAR	452	0.6 ± 0.1
GCGGCG (G_2)	442	0.3 ± 0.03
CGCCGC (C_2)	443	1.2 ± 0.1
$\{G_2\text{-}C_2\}$	475	1.1 ± 0.1
polyd(G-C)	480[c]	0.3 ± 0.03
polydG-polydC	471	
polyd(A-T)	481[c]	4.6 ± 0.4

[a] 1 mM cacodylate buffer pH = 6.0, 4 mM NaCl, [**1**] = 5 μM, T = 20 °C, the fluorescence maximum and yield of free **1** are, respectively, λ_{max}= (433 ± 1) nm and $\Phi_0 = (4.2 \pm 0.5) \times 10^{-3}$. [b] Limit values obtained in the presence of 5−10 molar excess of the oligomer over [**1**]. [c] Values measured in the presence of 100−300 molar excess in phosphate units.

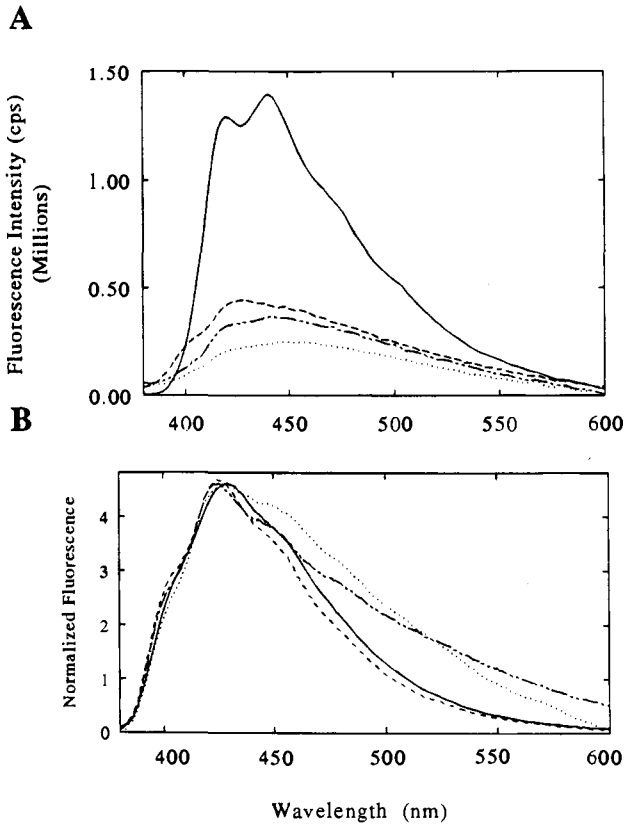

Figure 4. (A) Comparison of the fluorescence spectra of the macrocyclic acridine **1** bound to the hairpins studied; 4 mM NaCl, 1 mM cacodylate buffer pH = 6.0, [**1**] = 5 μM, excitation wavelength: 360 nm, excitation and emission slits: 1.15 nm; [hairpins] = 40 μM, full line: sA_3, broken line: sT_5, broken and dotted line: sA_5, dotted line: sTAR. (B) Comparison of the normalized fluorescence spectra of the macrocyclic acridine **1** complexed to T mono and oligomers; same conditions as in (A), full line: [UMP] = 50 μM, broken line: $[dT_4]$ = 40 μM, broken and dotted line: [polydT] = 20 μM; dotted line: $[sT_5]$ = 40 μM.

The λ_{max} similarity observed between adenine oligomers and the latter hairpins, distinct from that of **1** bound to the stem model $\{G_2\text{-}C_2\}$ as well as to other duplexes, lend, strong support to the single-stranded environment of **1** in the sA_3 and sA_5.

Moreover, Figure 4B shows that the macrocyclic acridine exhibits similar fluorescence maxima for T-rich oligonucleotides, including sT_5: $\lambda_{max} = (425 \pm 1)$ for dT_4 and polydT, $\lambda_{max} = (429 \pm 1)$ for UMP. If the 5 T of sT_5 are replaced by CTGGGA (sTAR), then the fluorescence maximum of **1** is observed at (452 ± 1) nm. These results show that the macrocyclic acridine is sensitive to the loop sequence and allow the assignment of the macrocycle acridine binding site to the loop of the sA_3, sA_5, sT_5, and sTAR hairpins.

(b) Stoichiometry of the Macrocyclic Acridine 1–sA_3 Complexes. The complexes between the macrocyclic acridine **1** and sA_3 have been further characterized by gel filtration on a Sephadex G-10 column. This technique allows the separation of oligonucleotides according mainly to their molecular weight, the larger ones being eluted earlier in the elution curve. Typical elution profiles of sA_3 solutions containing increasing [**1**] are compared to that of free sA_3 (Figure 5A). The elution volume of free sA_3 corresponding to the maximum OD monitored at 280 nm, is $V_{max} = (3.6 \pm 0.3)$ mL. The sA_3 solutions containing **1** are all eluted at $V_{max} = (2.8 \pm 0.3)$ ml, earlier than free sA_3. Comparable V_{max} values are observed independently of the [**1**]/[sA_3] ratios ranging from 1/4 to 5/1, but the $OD_{max}(280)$ values differ. These $OD_{max}(280)$ drop sharply at [**1**]/[sA_3] > 2. The same holds when the elution profile is monitored at 362 nm, the maximum of **1** absorption. The absorption and fluorescence spectra of the eluted fractions are consistent with the presence of complexed **1**.

The 280 nm wavelength mainly measures the oligonucleotide concentration ($\epsilon = 5.3 \times 10^4$ $M^{-1}\cdot cm^{-1}$), whereas 362 nm is the monitoring wavelength for the macrocyclic acridine. A unique complex between sA_3 and **1** should therefore be characterized by a single ratio OD(280)/OD(362) along the elution process. Figure 5B shows that it is indeed the case for all [**1**]/[sA_3] < 2 . If these ratios are larger or equal to 2, OD(280)/OD(362) is no more constant over the whole elution process. The fraction corresponding to OD_{max} is still eluted around 2.8 mL, similarly to the other ratios, indicating the presence of the same species. However, deviations from the usual OD(280)/OD(362) are clearly seen, especially at elution volumes above 3.0 mL, and the elution can only be completed after several column volumes.

These gel filtration results point out the existence of two kinds of sA_3–**1** complexes:

—The first one is characterized by a unique OD(280)/OD(362) ratio, leading to an extinction coefficient $\epsilon = (1.1 \pm 0.1) \times 10^4$ $M^{-1}\cdot cm^{-1}$, compatible with a 1/1 stoichiometry of this complex with respect to the value of free **1** ($\epsilon = (1.37 \pm 0.05) \times 10^4$ $M^{-1}\cdot cm^{-1}$),

—The second complex is only observed at or above a two-fold excess of **1** over sA_3. It adsorbs to the (G-10) polymer matrix, accounting for the large OD decrease. However, it can be eluted with large amounts of buffer solutions, suggesting an equilibrium between adsorbed and soluble species. It may be consistent with a 2/1 stoichiometry: such a complex should be neutral, since the eight negative charges of the phosphates of sA_3 are balanced by the 2 × 4 charges of the two macrocyclic acridine molecules. As indicated above, the second complex is present together with the first 1/1 one.

(c) Binding Constants of the Macrocyclic Acridine to the sA_3 Hairpin and the dA_3 Trimer. The above experiments point out at the existence of two complexes, which are not disrupted by gel filtration, qualitatively implying large binding constants of **1** to sA_3. However, the adsorption of the 2/1 complex preclude the quantitative determination of its binding constant by spectroscopic methods. The existence of this second

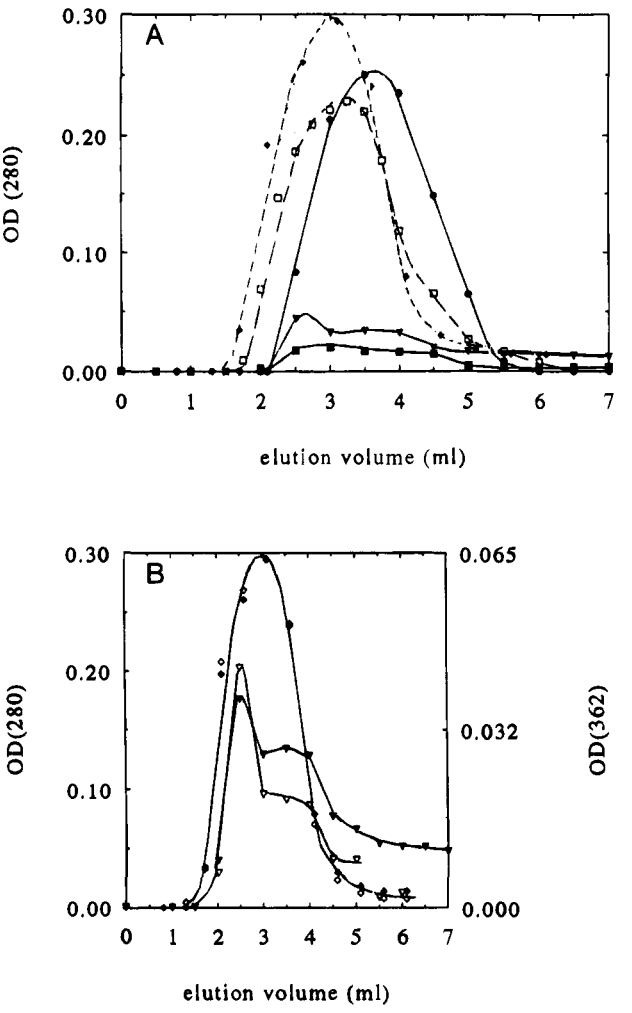

Figure 5. (A) Effect of macrocyclic acridine **1** concentration on the elution profiles of sA_3 on a Sephadex G-10 column, monitored at 280 nm; eluant: cacodylate buffer pH = 6.0, [sA_3] = 10 μM; full circles: sA_3 alone, open squares: [**1**] = 2.5 μM, full diamonds: [**1**] = 10 μM, full triangles: [**1**] = 20 μM, full squares: [**1**] = 50 μM. (B): Stoichiometry of the sA_3–macrocyclic acridine complex(es); same conditions as in part (A), full and open diamonds: [**1**] = 10 μM monitored at 280 nm (left scale) and 362 nm (right scale) respectively, full and empty triangles: [**1**] = 20 μM monitored at 280 and 362 nm, respectively, expended four times relative to both left and right scales.

complex renders difficult the determination of the binding constant K_1 of the first one at 1/1 stoichiometry. We used [sA_3] = (3–10) μM in 100–1000 fold molar excess over **1**, conditions that favor the formation of the 1/1 complex C_1.

$$\text{hairpin} + \mathbf{1} \overset{K_1}{\rightleftharpoons} C_1 \qquad (1)$$

In these experimental conditions, the sA_3 hairpin is the only structure in solution containing **1**, based on fluorescence spectra, although the free oligonucleotide itself is partly in the bulged duplex form at 25 °C and [sA_3]= 10 μM. The bound macrocyclic acridine presents a limiting fluorescence spectrum similar in vibronic structure and yield to that of figure 2a providing excess [sA_3] over [**1**]. The binding constant K_1 is determined by monitoring sA_3 absorbance changes at 257 nm, the large excess of sA_3 over **1** insures a negligible contribution of **1** absorption. Reverse titration results for sA_3 hairpin lead to the binding constant $K_1 = (4.5 \pm 0.5) \times 10^7$ M^{-1}. The 1/1 stoichiometry, resulting from the gel filtration experiments, is confirmed by the fit of the data according to eq 1.

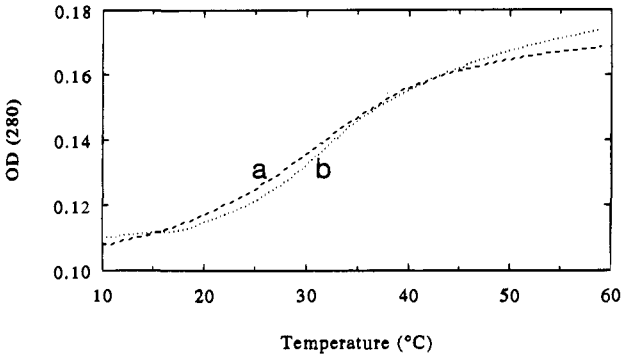

Figure 6. Comparison of the melting profiles of $\{G_2C_2\}$ oligomer alone and in the presence of macrocyclic acridine **1**. a: $[\{G_2C_2\}] = 2\ \mu M$ in double strand, b: in the presence of $[\mathbf{1}] = 2\ \mu M$, 4 mM NaCl, 1 mM cacodylate buffer pH = 6.0.

Table 2 : T_m Values and Related Thermodynamic Parameters of the Hairpin to Coil Transition of sA_3 in the Presence of Macrocyclic Acridine **1** at 4 mM NaCl, 1 mM Cacodylate Buffer, pH = 6.0 Assuming a Two-State Model

[1]/[sA_3] (M strand/M)	T_m (°C)	ΔT_m (±2 °C)	$-\Delta H$ (Kcal/mol)	$-\Delta S$ (eu)	$-\Delta G$(25 °C) (Kcal/mol)
free sA_3	47 ± 1		19 ± 2	59 ± 5	1.4
1/4	47 ± 1				
1/2	49 ± 1	2			
1/1	57 ± 2	10			
2/1	67 ± 2	20			
4/1	70 ± 2	23			
5/1	75 ± 2	28	38 ± 3	108 ± 10	5.7

The value of K_1 is almost two orders of magnitude higher than the binding constant determined for the trimer dA_3, $K = (6 \pm 1) \times 10^5\ M^{-1}$ by fluorescence spectroscopy. This difference in affinity between dA_3 and sA_3 possessing the A_3 binding site emphasizes the selectivity of the macrocyclic acridine **1** for the hairpin loop structure over "random" single-strand.

(d) Melting Profiles of sA_3 and $\{G_2\text{-}C_2\}$ in the Presence of 1. 1. Melting Temperature of the Duplex $\{G_2\text{-}C_2\}$ in the Presence or Absence of 1. Figure 6 shows similar T_m values obtained for the model duplex $\{G_2\text{-}C_2\}$, with and without **1**. This comparison points out that the macrocyclic acridine does not stabilize the double helix unlike intercalators including acridine derivatives.

2. Effect of the Stoichiometry [sA_3]/[1] on sA_3 Melting Temperature. Table 2 summarizes the results obtained at 4 mM NaCl, [sA_3] = 10 μM in the presence of different macrocyclic acridine concentrations. The curves are reversible, and an isosbestic point is observed at (260 ± 1) nm between 55 and 90 °C, [**1**]/([sA_3] ranging from 2/1 to 1/2, [sA_3] = (1−10) μM.

A clear dependence of T_m2 on the [**1**]/[sA_3] ratio is observed. Excess sA_3 over **1** does not displace T_m2 compared to free sA_3. In contrast, large T_m2 shifts ranging from 20 to 28 °C are obtained at [**1**]/[sA_3] ≥ 2 (Figure 7, curves b and a). A decrease of the initial absorbances at low temperatures is also observed at 280 nm compared to free sA_3. These relative OD decreases are larger when [**1**] increases. They may be related to the gel filtration results: a larger [**1**] at constant [sA_3] increases the proportion of the 2/1 complex, part of which may be adsorbed on the cell walls as in the case of the G10 polymer.

3. Comparison of the Melting Temperature of sA_3 in the Presence of the Macrocyclic 1 and Monomeric 2 Compounds. The T_m2 shift observed in the presence of **1** does not show up if the macrocyclic compound is replaced by two

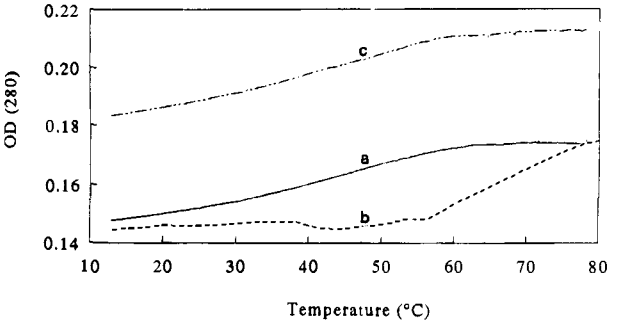

Figure 7. Melting profiles of sA_3 in the presence or absence of the macrocycle **1** and the monomeric acridine **2**; [sA_3] = 2.8 μM, 4 mM NaCl, 1 mM cacodylate buffer pH = 6.0, a: free sA_3, b: [**1**]/[sA_3] = 2, c: [**2**]/[sA_3]= 4.

equivalents of the monomeric acridine **2** (Figure 7 curves c and b). This implies that the macrocyclic structure of **1** is needed for hairpin stabilization.

Discussion

1. Comparison of the Thermodynamic Parameters of sA_3 to those of Related Hairpins. The biphasic melting profiles of sA_3 offer experimental evidence that such a partly-complementary oligomer can adopt both the hairpin and the bulged duplex conformations. The slow duplex to hairpin interconversion did not allow its characterization at the low ionic strength used.[57] T_m2 of the intramolecular hairpin to coil transition remains constant despite the 50 fold increase in strand concentration.

The thermodynamic parameters derived from the melting curves assuming a two-states model are $\Delta H = -(19 \pm 2)$ Kcal/mol and $\Delta S = -(59 \pm 5)$ eu. The experimental ΔH is smaller than the calculated value at 1 M NaCl from the nearest-neighbor approximation assuming no contribution of the loop, $\Delta H = -23$ Kcal/mol. The measured ΔH value is smaller than that observed for the corresponding hairpin with a five-membered adenine loop A_5 ($\Delta H = -23.5$ Kcal/mol).[61] This increase in ΔH with the loop size, in contrast to the enthalpic decrease observed with other hairpins that possess longer stems than sA_3,[13,16,34,36,60,62] suggests that the innermost GC pair is likely to be partially altered. This pair is probably partly disrupted since two GC pairs are not sufficient in $GC(A)_4GC$ to form a hairpin.[32] This is also supported by the strong alteration of the stem structure for small hairpin loops demonstrated by enzymatic cleavage.[16,60]

2. The Complexes between the Macrocyclic Acridine 1 and sA_3. The macrocyclic acridine **1** forms two distinct complexes with the hairpin studied. These complexes present different elution profiles in gel filtration: the 1/1 complex is eluted earlier compared to the free hairpin, whereas the 2/1 complex elution is smeared. The latter complex is responsible for the adsorption phenomena observed with different techniques: gel filtration, spectroscopic measurements obtained at similar **1**/sA_3 ratios independently of the technique used. This 2/1 complex has a low solubility in aqueous solutions, since it is uncharged.

The binding site of the macrocyclic acridine in the 1/1 complex is within the hairpin loop as suggested by fluorescence spectroscopy (see below). The possible binding sites of the two macrocyclic acridine molecules in the 2/1 complex may be evaluated in terms of accessibility: more accessible residues within the hairpin structure may represent more favorable

(61) Gavriatopoulos, I.; Slama-Schwok, A. unpublished data.
(62) Erie, D. A.; Suri, A. K.; Breslauer, K. J.; Jones, R. A.; Olson, W. K. *Biochemistry* **1993**, *32*, 436−454.

binding sites. This accessibility varies within hairpin families bearing a common stem sequence and X_n loops. For A_3 loops (X = A, n = 3), an enzymatic cleavage study shows that the main cleavage site is the second adenine residue from the 5′ side of the loop. Minor sites lie at the loop stem junction (last base pair close to the loop and first A residue both at the 5′ loop extremity),[60] consistent with the perturbation of the sA_3 stem structure derived from the thermodynamic parameters mentioned above. This alteration, observed for small loops, n = 3 to 4 residue, is limited to 2−3 base pairs closest to T_3 or A_4 loops.[16] The stem-loop junction could thus be the binding site of the second macrocyclic acridine molecule in the 2/1 complex, whereas the first one should be within the loop.

An alternative interpretation could also be entertained for the 2/1 complex binding site. It has been shown that bis-intercalators with extended and rigid linkers are able to intercalate intermoleculary, with each one of the aromatic subunits located in separate duplexes. This binding mode yields to DNA cross-links that aggregate with different sizes and shapes and thus electrophoretic mobilities.[55b,c] The flexibility of the linkers of **1** allows their extension and the "unfolding" of the macrocycle which then becomes an almost flat molecule. This form could bind to two different hairpin molecules, inducing cross-linking between the two. However, this interpretation predicts a stoichiometry of three macrocycles per two hairpins, in contrast with the 2/1 one found by gel filtration; it is possible that an additional bisacridine **1** is needed for this cross-linking to occur in order to overcome the electrostatic repulsion of the phosphates, especially at the low ionic strength used. More work is needed to assess precisely the binding site of the second macrocycle in the 2/1 complex.

3. The Macrocyclic Acridine 1: a Potential Fluorescent probe of Oligonucleotide Structure that Discriminates between Single- and Double-Helical DNA. The study of the fluorescence spectra of **1** bound to model single- and double-stranded oligomers and polynucleotides enables the correlation of the macrocyclic acridine spectral modifications to sA_3 different structures, hairpin or bulged duplex. The similarity in fluorescence maximum for adenine oligomers and the sA_3 and sA_5 hairpins permits the assignment of the binding site of the macrocyclic acridine in the 1/1 complex to the adenine(s) loop. A similar comparison can be done between sT_5 and thymine containing oligonucleotides, leading to the same conclusion. Moreover, the binding of **1** on the studied hairpins, designed to possess a variable loop and a common stem, is evidenced by the change in **1** fluorescence maximum according to the loop sequence. This assignment of the 1/1 complex binding site to the loop also relies on the difference in λ_{max} observed for the stem model duplex and sA_3 hairpin.

The red-shifted shoulder of **1** bound to sA_3 bulged duplex is observed at a similar wavelength to the characteristic peak of **1** on double-stranded DNAs, although the fluorescence maximum still peaks at 442 nm (Figure 2b). The value of λ_{max} hints to an adenine environment close to a double-helical structure. In other words, the binding site of **1** may be the bulged adenines in sA_3 duplex structure. More work is needed to assess this assignment. The T_m data support the above assumption that intercalation in the G-C paired stem is not a favored binding site for **1**.

It is interesting to note the variations in relative fluorescence yield observed between the series AMP, dA_3, dA_4, dA_{20}, and sA_3 hairpin. The fluorescence yield of the former complexes is significantly lower than for the sA_3 hairpin loop. This difference may result from a different stacking pattern, namely the adenine self-stacking in the hairpin loop varies from that present in dA_n oligomers. Other related structural parameters may also explain the difference in fluorescence yield between sA_3 hairpin and dA_3, such as the distance between consecutive adenines. It could be larger in the former in order to close the A_3 loop that in the unconstrained dA_3 oligomer.[16,34,60,62] This may induce the flexible cavity of the macrocyclic acridine to open up to accommodate to this larger interresidue distance. The increase in the interchromophoric distance by electrostatic repulsion between protonated acridinium moieties at pH = 2, enhances markedly the fluorescence yield of **1** compared to that of uncharged ones at pH = 6.0. This fluorescence enhancement does not arise from the difference in yield between uncharged acridine and acridinium chromophores since the variation of the model (monomeric) compound **2** with the pH does not present such an effect. It supports the above difference in adenine distance between dA_3 and sA_3 loop evidenced by the response of **1** fluorescence yield. Such a difference in structure may explain the higher binding constant by almost two orders of magnitude of the macrocyclic acridine **1** to sA_3 hairpin compared to that with the trimer dA_3.

The relative fluorescence yield of the bisacridine is much lower when bound to sA_5 than to sA_3. This difference may be related to a more extensive stacking in sA_5, resulting in a smaller gap between consecutive adenines needed to close the A_5 loop than the A_3 one. The larger stem alteration in sA_3 relative to that of sA_5 may also alter the loop stacking more extensively in the former than in the latter. The variation in the extent of stacking may explain the large decrease in the fluorescence yield of the macrocyclic acridine, with low self-stacking dT_4 and polydT relative to sT_5, consistent with an ordered T_5 loop. These interpretations are consistent with a simulation study of A_5 and T_5 loops, predicting that both structures are highly ordered, with a high degree of base stacking.[62]

This sensitivity to DNA structure seems to be unique to the macrocyclic acridine **1**. The model acridine compound **2** does not present marked λ_{max} shifts of its fluorescence spectrum in the presence of single- and double-stranded polynucleotides as it is the case for the macrocyclic acridine (data not shown). Acridine derivatives are well-known intercalators into double helices but bind weakly to single-stranded DNA.[63] The spectral sensitivity of **1** to the DNA secondary structure is specific to this compound and probably results from its macrocyclic structure.

4. Selective Stabilization of the Hairpin Structure by the Macrocyclic Acridine 1. T_m data show that the macrocyclic acridine induces a 25 °C shift of the hairpin to random coil transition at 2/1 and higher **1**/sA_3 ratios, quantified as $\Delta\Delta G$(25 °C)= −4.3 Kcal/mol. This T_m displacement is specific to the hairpin structure since no stabilization is observed for the {G_2-C_2} duplex in contrast with the T_m shift of double helixes induced by intercalators including acridine derivatives and bisintercalated bisacridines.[54] The shorter length of the diethylenetriamine linker of **1** compared to the spermine one of the macrocycle synthesized by Zimmerman and co-workers may allow a switch from a nonintercalative to a bisintercalative binding mode. The linker length is one of the critical parameters that governs bisintercalation.[52,53]

The hairpin melting temperature is not increased when **1** is replaced by the model acridine compound **2**. This implies a relationship between the structure of these compounds and their ability to stabilize the sA_3 hairpin form. The high affinity and selectivity of the macrocyclic acridine **1** for the hairpin structure may result from the macrocyclic structure, which as noted above was designed with the expectation that it would induce

(63) Dourlent, M.; Hélène, C. *Eur. J. Biochem.* **1971**, *23*, 86−95.

preferential binding to single-stranded domains. The flexibility of the bis-cationic polyammonium linkers may also favor **1** binding to the three-membered loop. NH_4^+ ion was shown to stabilize rRNA tertiary structure, the bases essential for this effect being within or surrounding the junction loop.[64]

It is probable that the 2/1 complex contributes to the overall T_m shift. The location at the loop−stem junction assumed for the second macrocyclic acridine molecule in the 2/1 complex seems consistent with such a hairpin stabilization.

The thermal stabilization of the macrocyclic acridine hairpin complex ΔT_m relative to the free hairpin follows the equation: $\Delta T_m = [(T°_m \cdot T_m)/(nR\Delta H)] \times \ln(1 + K.a_L)$ where $T°_m$ and T_m are the transition temperatures of the free sA_3 and of the complex respectively; ΔH, the dissociation enthalpy of the loop that constitutes the ligand binding site; n, the apparent number of ligand per binding site, and a_L, the activity of the free ligand at $T = T_m$, assumed equal to half of the total ligand concentration.[65] Enthalpic contributions of four-membered DNA loops have been reported[31,37,40] with values ranging from $\Delta H = -3.3$ to -11.1 kcal/mol for GATC(A_4)GATC and GATC(GAAA)GATC, respectively.[31] Based on the calculated $\Delta H = -23$ Kcal/mol and the measured $\Delta H = -19$ Kcal/mol, the loop enthalpy of formation should be $\Delta H_{loop} = -4.0$ Kcal/mol, a value closer to that reported for the above A_4 loop. The corresponding calculated binding constants are $K = 1 \times 10^7$ and 7×10^7 M^{-1} assuming $n = 1$ and $n = 2$ respectively. The measured value $K_1 = (4.5 \pm 0.5) \times 10^7$ M^{-1} lies in the same order of magnitude.

5. Comparison of the Binding of the Bisacridine to sA_3 and dA_3. The macrocyclic acridine presents an 80 times higher affinity for the sA_3 hairpin over the single-stranded oligomer dA_3. Such an effect may be related to the structural differences between sA_3 and dA_3 as mentioned above. It is possible that the disruption of the adenine self-stacking needed to accommodate dA_3 costs more in energy than the increase of **1** interchromophoric distance necessary to fit to sA_3 loop.

(64) Wang, Y. X.; Lu, M.; Draper, D. E. *Biochemistry* **1993**, *32*, 12279−12282.

(65) Crothers, D. M. *Biopolymers* **1971**, *10*, 2147−2160.

Conclusion

The macrocyclic acridine **1** forms two complexes of 1/1 and 2/1 stoichiometries, with the sA_3 hairpin. A high affinity constant of the macrocycle for the sA_3 hairpin in the 1/1 complex is obtained, $K_1 = (4.5 \pm 0.5) \times 10^7$ M^{-1}. The macrocycle binding site is expected to lie within the hairpin loop to account for the fluorescence data on sA_3 and model oligomers. The same loop also constitutes the bisacridine binding site in sA_5, sT_5, and sTAR hairpins, based on a similar reasoning.

In contrast to the clear melting temperature displacement of the hairpin to coil transition, $\Delta T_m 2 \geq 25$ °C relative to free sA_3, the lack of T_m shift of the $\{G_2\text{-}C_2\}$ model duplex illustrates that the macrocyclic acridine does not stabilize the double helical structure, but specifically the hairpin. The comparison of **1** binding constants for dA_3 and sA_3 further demonstrates the selectivity of the macrocyclic acridine for the hairpin structure. This selectivity probably arises from the macrocyclic structure of the bisacridine **1** by comparison to the model acridine **2**.

Acknowledgment. This work was supported by a grant from The Agence Nationale de Recherches sur le Sida (to A.S.S). Dr. H. Porumb is acknowledged for helpful discussions, Prof. W. Olson for sending her hairpins coordinates, and T. Bataille for the drawings.

JA943803T